03

The grazing incidence reflection coefficient measurement with the usage of single channel scheme

© P.S. Antsiferov[1], L.A. Dorokhin[1], V.M. Makarova[1,2]

[1] Institute of Spectroscopy, Russian Academy of Sciences, Troitsk, Moscow, Russia
[2] National Research University Higher School of Economics, Moscow, Russia

e-mail: ants@isan.troitsk.ru

Received April 13, 2023
Revised April 13, 2023
Accepted May 12, 2023

The measurement of the grazing incidence reflection coefficient is one of the main methods of the evaluation of materials' optical constants in extreme ultraviolet spectral range. The present work describes a single channel method of such measurement, where the direct and reflected radiation, dispersed in a grazing incidence spectrometer, has been detected simultaneously by means of CCD matrix. The algorithm of the spectrograms processing, based upon the usage of the spectral modulation function, has been proposed. The elaborated method has been applied to the silicon reflection coefficient measurements at 5° grazing incidence in the spectral range 8−25 nm. The Quasi-Flat Field spectrometer and fast capillary discharge have been used in the experiment.

Keywords: Extreme ultraviolet, grazing incidence, reflection coefficient, capillary discharge.

DOI: 10.61011/EOS.2023.08.57284.4846-23

Introduction

Experimental studies in the extreme ultraviolet range of $\lambda \sim 10$ nm (EUV) are associated with a number of specific problems. The main difficulties lie in the strong absorption of such radiation by the substance and the low reflectance at normal incidence. However, practical applications in nanolithography [1] are causing a permanent increase in interest in this range. The development of EUV optical elements needs information about the optical properties of materials. One of the main methods for getting such information is to measure the grazing incidence reflectance.

Currently, the most accurate technique for determining the reflectance is based on the use of a reflectometer with synchrotron radiation as an EUV source. The choice of such a source is associated with high stability and reproducibility, which provides measurement accuracy better than 1%. Thus, the team of the Helmholtz-Zentrum Berlin has developed a reflectometer for the BESSY-II synchrotron [2] to study the properties of nanooptical elements in the UV and EUV ranges. Additional capabilities of BESSY-II are discussed in the article of the Physikalisch-Technische Bundesanstalt [3]. A similar setup [4] was implemented on the basis of the ALS synchrotron radiation source in California. An example of the use of spectral and angular dependences of the reflectance to determine optical constants of materials is [5].

However, practical needs have also led to the development of techniques for measuring reflectance using compact laboratory radiation sources. In [6], the reflection of thin films was measured using a laboratory gas-discharge source of EUV radiation. In [7], the reflectance of the sample was also determined using gas pinch as a radiation source. In the Institute of Physics of Microstructures of the Russian Academy of Sciences, a reflectometer with a source based on laser plasma was developed [8,9], which was used to test optical elements with multilayer coatings in a wide range of incidence angles.

The use of CCD matrices to record EUV radiation makes it possible to implement a simple single-channel scheme for measuring the grazing incidence reflectance [10]. Instead of the traditional monochromatization of the radiation with a continuous (quasi-continuous) spectrum, here the line spectrum of radiation transmitted and reflected from the sample is simultaneously recorded (Fig. 1), for which purpose the sample under study is placed inside a grazing incidence spectrometer. By measuring the reflectance at various spectral lines, its spectral dependence can be obtained. If not the total intensity at the maximum of spectral lines but the difference between it and the recorded intensity in a certain point at the base of the line is used as the measured quantity, then we can effectively get rid of all contributions continuous over the spectrum, including contributions from high diffraction orders. This study describes a technique for processing spectrograms of transmitted and reflected radiation, which uses building up of a spectral modulation function for each line. This technique makes it possible to most fully extract information from experimental spectrograms and achieve an accuracy of reflectance measurement of about 1%. The technique was used to process the results of an experiment to measure the reflectance of a silicon sample.

Experiment

The study presents the results of measurements of the reflectance from a silicon sample at a grazing angle of 5°.

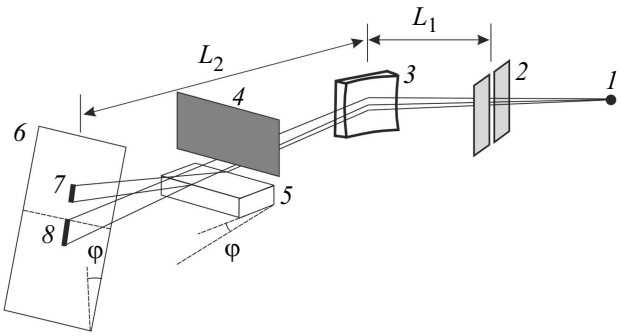

Figure 1. Scheme of the single-channel technique to measure the grazing incidence reflectance. *1* — EUV radiation source, *2* — entrance slit, *3* — spherical diffraction grating, *4* — bladed diaphragm, *5* — sample, *6* — plane of recording, *7* — reflected part of the radiation, *8* — transmitted part of the radiation.

The general measurement scheme is described in [10] and shown in Fig. 1. In the grazing incidence spectrometer used the Quasi-Flat Field scheme [11] is applied. In this scheme, the focusing surface of spectral lines is normal to the line of sight due to the shift of the entrance slit from the Rowland circle. The spectrometer uses a spherical diffraction grating with a radius of curvature of $R = 1$ m, a groove density of 1200 grooves/mm and an entrance grazing angle of 3°, entrance slit size of $20\,\mu$. According to [11], the distance from the entrance slit to the center of the grating is $L_1 = 22$ mm, the distance from the center of the grating to the plane of recording is $L_2 = 296$ mm. This value of L_2 is sufficient to accommodate a reflective sample with dimensions of the order of a few centimeters. A fast capillary discharge [12], with argon at a pressure of 80 Pa as working gas was used as a radiation source. The maximum discharge current of 40–50 kA is sufficient to excite the spectral lines of argon ions up to Ar IX. An example of the working spectrum is shown in Fig. 2. The lines were identified according to the data of [13]. A Greateyes GE 2048 512 BI CCD camera was used to record the spectra. Working size of the matrix was 27.6×6.9 mm, pixel size was $13.5 \times 13.5\,\mu$. A fragment of the spectrogram of the source radiation is shown in Fig. 3. In order to simultaneously register direct and reflected radiation, the camera was oriented with the long side of the matrix perpendicular to the direction of dispersion (Fig. 3). In this case, the simultaneously recorded range of wavelengths narrowed, and to study the reflectance in the entire working spectral range (8–25 nm), the camera was moved along the direction of dispersion.

In Fig. 3, *a*, the image corresponds to the radiation spectrum without a sample and without a bladed diaphragm inside the spectrometer (Fig. 1), the image in Fig. 3, *b* corresponds to the case of spectrometer with a sample and with a diaphragm. When a sample is placed, the transmitted radiation $A'B'$ corresponds to the section AB, the section $D'C'$ of the reflected radiation corresponds to the section CD on the spectrogram without the sample. To compare the transmitted and reflected radiation, we used sections of the spectrogram marked in Fig. 3 with numbers *1′* and *2′*.

Measurement procedure

When a sample is placed in the spectrometer during the experiment, the matrix records the time-integrated spectra of reflected and transmitted radiation. The spectral intensity profile for each line (I) consists of the spectral line itself (S) and the continuous background (B) (Fig. 4). The background radiation includes the detector dark current, the scattered radiation, and continuous contributions from the first and higher orders of diffraction. Due to the different values of the reflectance for radiation of different diffraction orders, the level of background intensity will make a disproportionate contribution to the intensity of transmitted and reflected radiation, which is the main difficulty in processing the spectrograms. There is no possibility to control the background radiation in the scheme used, therefore, to determine the reflectance for each spectral line, the background contribution must be subtracted from the recorded intensity.

It is proposed to solve this problem using the spectral modulation function (SM). To build up the function, it is necessary to take the difference between the maximum value of the intensity profile and the remaining points of the profile, i. e.

$$SM(\lambda) = I(\lambda_0) - I(\lambda), \tag{1}$$

where λ is spectral coordinate, λ_0 is position of the maximum. The form of the spectral modulation function for reflected (SM_r) and transmitted (SM_d) radiation is shown in Fig. 4.

Let us consider the use of the spectral modulation function to determine the reflectance. The background is assumed to be changing weakly across the spectral line

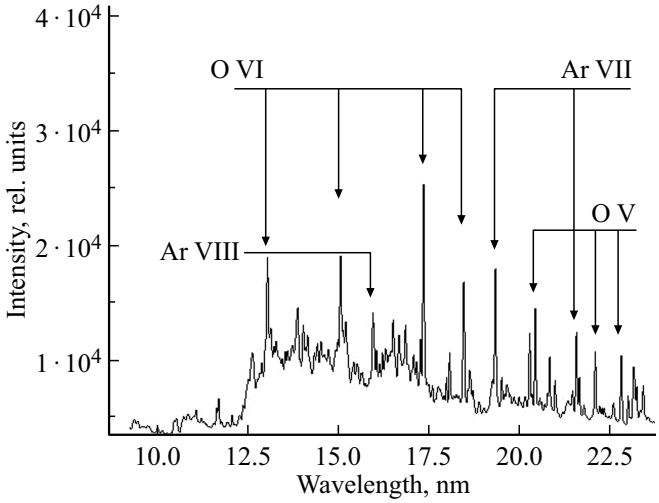

Figure 2. An example of an EUV spectrogram of the source. Marked lines are identified according to [13].

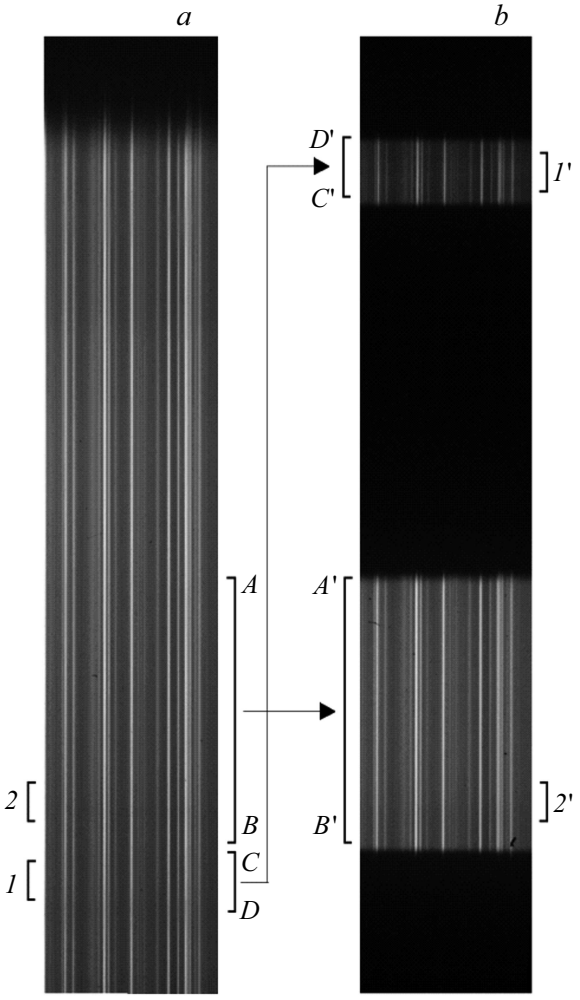

Figure 3. Image of spectral lines obtained using a CCD matrix in the range of 20–23 nm: *a* — without a sample and without a bladed diaphragm inside the spectrometer, *b* — with a sample and a diaphragm.

width, i.e. $B = \text{const}$. Then the intensity profile has the following form:

$$I_r(\lambda) = S_r(\lambda) + B_r, \quad I_d(\lambda) = S_d(\lambda) + B_d,$$

where d, r are referred to transmitted and reflected radiation, respectively. It follows from this that

$$SM_r(\lambda) = S_r(\lambda_0) - S_r(\lambda), \quad SM_d(\lambda) = S_d(\lambda_0) - S_d(\lambda). \tag{2}$$

Assume R is reflectance for a given spectral line. Then, according to (2), the spectral modulation functions of reflected and transmitted radiation are proportional to each other with a proportionality coefficient of R:

$$SM_r(\lambda) = R\, SM_d(\lambda).$$

Based on the above considerations, an algorithm was developed that makes it possible to determine the reflectance from experimental spectra. Fig. 5, 6 show an example of processing the spectral line at 22.7 nm (ion OV $2p^2 - 2p(^2P^0)3s$). The peculiarity of dealing with a real experimental spectrum is that the intensity profile consists of discrete values (Fig. 5, *a*), which correspond to pixels of the CCD matrix. The spectral coordinates of the measured points on the spectrograms of reflected and direct radiation do not coincide with each other due to the fact that the lines of the CCD matrix are not exactly perpendicular to the direction of dispersion. In this regard, the proposed algorithm uses additional steps, such as drawing an approximation curve to determine the maximum of the spectral line for reflected and transmitted radiation (Fig. 5, *b, c*) and interpolating the points of experimental intensity values (Fig. 6, *a*).

1. *Determining maximum of the spectral line*

The maximum intensity value from a discrete set of experimental points may not coincide with the real maximum of the spectral line profile. To determine the maximum, a third-order curve is drawn through several points with the highest intensity using the least squares method. We believe that to take into account the possible asymmetry of the intensity profile, a polynomial of the third degree is sufficient. Coordinates of the vertex of the approximation curve are selected (Fig. 5, *b, c*) as the coordinate of the corresponding λ_0 and the maximum intensity value of the spectral line $I_{r,d}(\lambda_0)$. To establish correspondence between the spectral profiles of direct and reflected radiation, the coordinates of individual spectral points are measured from the positions of maxima of the spectral lines (Fig. 6).

2. *Interpolating the profile of spectral line*

Coordinates of spectral points of the reflected and transmitted radiation do not coincide. Therefore, to compare the intensities of the spectra of reflected and transmitted radiation at points with the same wavelength, it is necessary to interpolate the points of the experimental spectra. For this purpose, splines are built up which then are used to supplement the points of the reflected radiation spectrum with intensities at points corresponding to the transmitted radiation spectrum, and vice versa (Fig. 6, *a*).

3. *Building up the spectral modulation function*

Following (1), a spectral modulation function is built up: each point of the intensity graph (taking into account the interpolated values, Fig. 6, *a*) is assigned the value of the difference between the maximum value of the spectral line and the intensity value at the point. The spectral modulation graph is shown in Fig. 6, *b*.

4. *Determining the reflectance*

The reflectance R is fitted using the least square method:

$$\sum_i (R\, SM_d^i - SM_r^i)^2 \to \min. \tag{3}$$

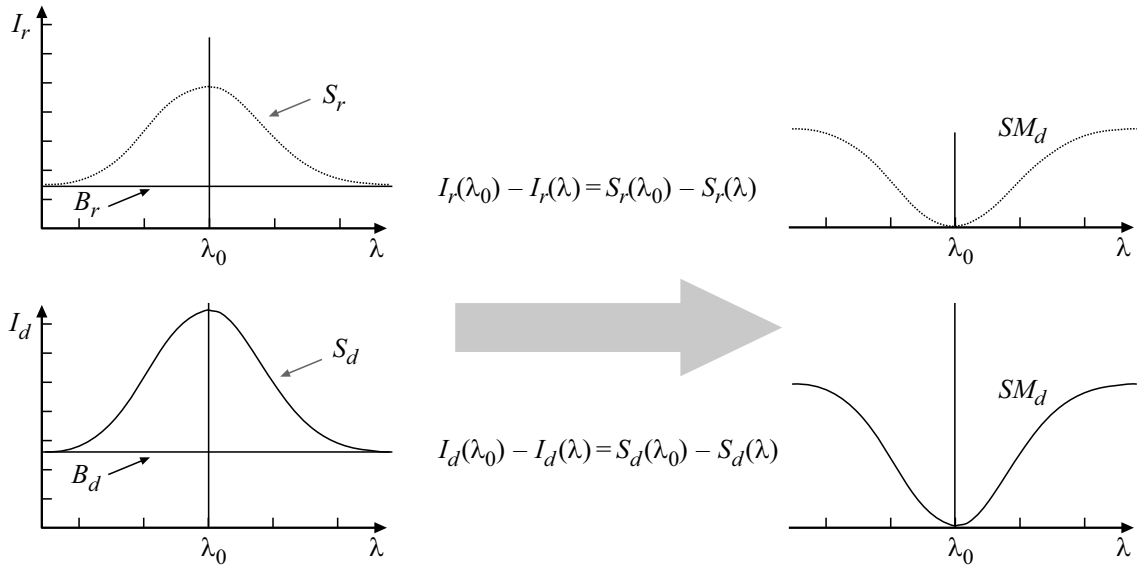

Figure 4. Scheme for building up the spectral modulation function.

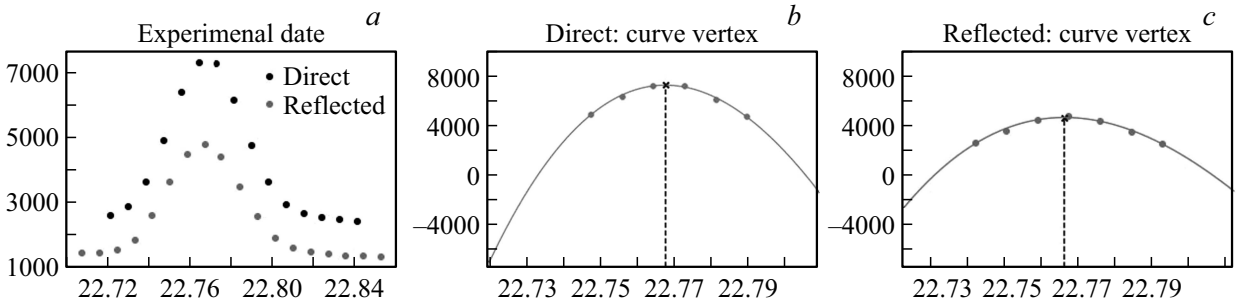

Figure 5. Stage 1 of processing the spectral line at 22.7 nm. *a* — experimental values; *b, c* — building up of a 3-rd order approximation curve.

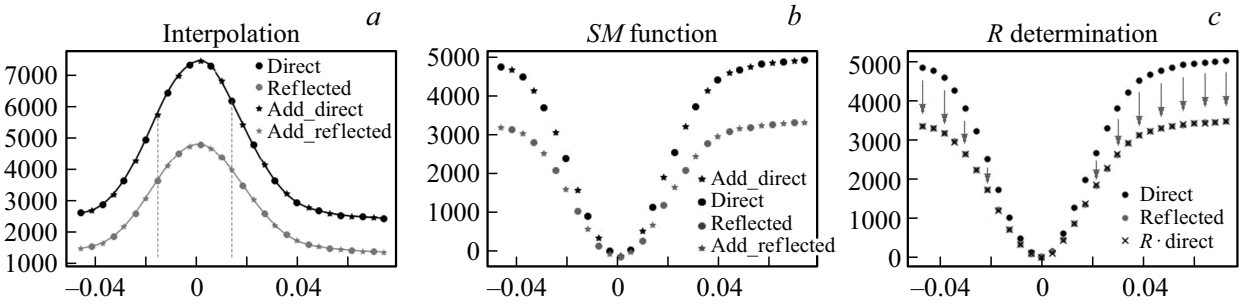

Figure 6. Stages 2–4 of processing the spectral line at 22.7 nm. *a* — splining and interpolating the spectral profile of the line; *b* — building up the spectral modulation function; *c* — determining the reflectance.

The optimal value of R, according to (3), is taken as the measured reflectance (Fig. 6, *c*).

Results and discussion

Using the developed algorithm, the experimental data of measuring the reflection from a silicon sample at a grazing angle of 5° in the spectral range of 8–25 nm were processed. The spectral dependence of the reflectance resulted from the processing is presented on the graph (Fig. 7). Each point of the graph is obtained by averaging over 3–5 independent measurements. The shown errors correspond to 3σ. The graph compares the experimental values with the data from the CXRO database [14] for silicon reflectance. The best agreement between the graphs is achieved when an additional SiO_2 layer with

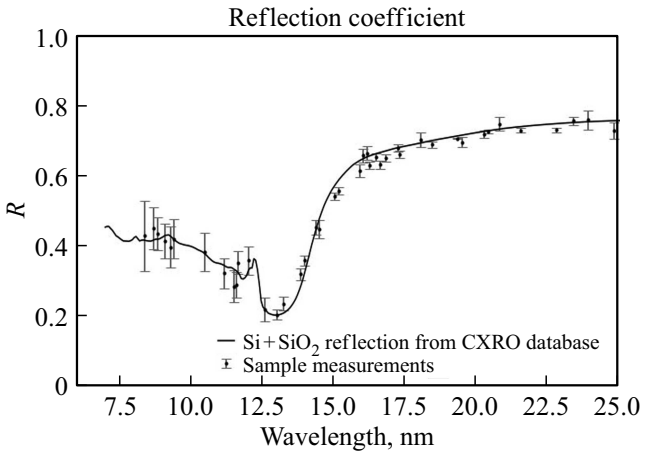

Figure 7. Spectral dependence of the silicon reflectance in the range of 8–25 nm. Dots — measured value, curve — data of the CXRO database [14].

a thickness of 4 nm on the silicon surface is taken into account.

The average spread of experimental points relative to the CXRO data is at the level of a few percent. The measured values reproduce the region of anomalous silicon dispersion.

The sensitivity of the CCD matrix drops by 2 times in the wavelength region of $\lambda < 13$ nm [15], which can be seen from the spectrogram shown in Fig. 2. The increase in the error of points on the graph (Fig. 7) associated with this fact is determined by the Poisson statistics of the number of radiation quanta absorbed in one pixel of the CCD detector. To achieve an accuracy of about 1%, it is necessary to increase the number of measurements several times or use a more intense radiation source.

One of systematic error sources is the astigmatism of the spectrometer. The intensity of the spectral line image can vary along its direction due to the possible non-parallelism of the slit blades and the inhomogeneity of the grating reflection along the grooves. The radiation transmitted and reflected from the sample corresponds to different parts of the spectral line image. Numbers in Fig. 3, *a* indicate the areas of the spectral line corresponding to the areas of reflected (*1*) and transmitted (*2*) radiation. To take into account the above-mentioned effect of astigmatism, it is necessary to compare spectrograms for sections *1* and *2*. For these sections, a procedure similar to the determination of R by the above algorithm is carried out; the values obtained for different lines are averaged. In our case, this correction amounted to 3%.

The second source of systematic errors is the spatial heterogeneity of the matrix sensitivity. To take this into account, an additional experiment was carried out to create uniform illumination of the CCD matrix. An EUV radiation source (vacuum spark, $C = 0.01\,\mu$F, $U = 10$ kV) with a size of about 1 mm was located at a distance of 1 m from the CCD matrix. This distance guaranteed uniform illumination of the CCD matrix within 0.02%. The intensity distribution over its surface was recorded. In this case, signals from the areas corresponding to the positions *1′* and *2′* in Fig. 3, *b* were compared. For our detector, this correction was about 2%.

Conclusion

The processing technique described in this study, together with the previously proposed single-channel scheme to measure the grazing incidence reflectance, represent the concept of a reflectometer relevant for the problem of determining the optical constants of materials in the EUV range. The maximum grazing angle is determined by the size of the CCD matrix and is 15–20°. The relative spectral width of the radiation at an individual point is determined mainly by the Doppler width of the lines emitted by the source plasma, and for the electronic temperature range of 10–50 eV it is of the order of $\delta\lambda/\lambda \sim 10^{-4}$. The tradeoff for the simplicity of the described technique is the inability to smoothly adjust the wavelength, which can be important for studying areas of anomalous dispersion. A possible solution for this problem would be to use other radiation sources, such as vacuum spark or laser plasma, for which a very wide selection of emitting chemical elements is available. In the available databases [13] one can find spectral lines of various ions in almost the entire EUV range.

Funding

This study was carried out under State assignment FFUU-2022-0005.

Conflict of interest

The authors declare that they have no conflict of interest.

References

[1] V.Y. Banine, K.N. Koshelev, G.H.P.M. Swinkels. J. Phys. D: Appl. Phys., **44** (25), 253001 (2011). DOI: 10.1088/0022-3727/44/25/253001

[2] F. Schäfers, P. Bischoff, F. Eggenstein,A. Erko, A. Gaupp, S. K?nstner, M. Mast, J.-S. Schmidt, F. Senf, F. Siewert, A. Sokolov, T. Zeschke. J. Synchrotron Radiat., **23** (1), 67–77 (2016). DOI: 10.1107/s1600577515020615

[3] B. Beckhoff, A. Gottwald, R. Klein, M. Krumrey, R. Müller, M. Richter, F. Scholze, R. Thornagel, G. Ulm. Phys. Status Solidi B, **246** (7), 1415–1434 (2009). DOI: 10.1002/pssb.200945162

[4] J.H. Underwood, E.M. Gullikson. J. Electron Spectrosc. Relat. Phenom., **92** (1–3), 265–272 (1998). DOI: 10.1016/s0368-2048(98)00134-0

[5] R. Ciesielski, Q. Saadeh, V. Philipsen, K. Opsomer, J.P. Soulié, M. Wu, P. Naujok, R. van de Kruijs, C. Detavernier, M. Kolbe, F. Scholze, V. Soltwisch. Appl. Opt., **61** (8), 2060–2078 (2022). DOI: 10.1364/AO.44715

[6] M. Banyay, L. Juschkin. Appl. Phys. Lett., **94** (6), 063507 (2009). DOI: 10.1063/1.3079394

[7] K. Bergmann, O. Rosier, C. Metzmacher. Rev. Sci. Instrum., **76** (4), 043104 (2005). DOI: 10.1063/1.1884387
[8] V.O. Dogadin, S.Yu. Zuev, N.N. Salashchenko, N.I. Chkhalo, A.V. Shcherbakov. J. Surf. Invest.: X-Ray, Synchrotron Neutron Tech., **9** (4), 726–734 (2015). DOI: 10.1134/s1027451015040072.
[9] S.A. Garakhin, I.G. Zabrodin, S.Y. Zuev, I.A. Kas'kov, A.Y. Lopatin, A.N. Nechay, V.N. Polkovnikov, N.N. Salashchenko, N.N. Tsybin, N.I. Chkhalo, M.V. Svechnikov. Quantum Electron., **47** (4), 385–392 (2017). DOI: 10.1070/qel16300.
[10] D.B. Abramenko, P.S. Antsiferov, L.A. Dorokhin, V.V. Medvedev, Y.V. Sidelnikov, N.I. Chkhalo, V.N. Polkovnikov. Opt. Lett., **44** (20), 4949 (2019). DOI: 10.1364/ol.44.004949
[11] P.S. Antsiferov, L.A. Dorokhin, P.V. Krainov. Rev. Sci. Instrum., **87** (5), 053106 (2016). DOI: 10.1063/1.4945654
[12] P.S. Antsiferov, L.A. Dorokhin. J. Appl. Phys., **113** (24), 243303 (2013). DOI: 10.1063/1.4811714
[13] *NIST Chemistry WebBook* [Electronic source]. URL: https://webbook.nist.gov/chemistry/
[14] *CXRO X-Ray Interactions With Matter* [Electronic source]. URL: https://henke.lbl.gov/optical_constants/
[15] *Greateyes* [Electronic source]. URL: https://www.greateyes.de/projects/greateyes/static/custom/file/greateyes_InVacuum_Camera_Series_Rev03.pdf

Translated by Y.Alekseev